

## Minimization of cochlear implant stimulus artifact in cortical auditory evoked potentials

Phillip M. Gilley<sup>a,\*</sup>, Anu Sharma<sup>a</sup>, Michael Dorman<sup>b</sup>, Charles C. Finley<sup>c</sup>,  
Arunachalam S. Panch<sup>a</sup>, Kathryn Martin<sup>a</sup>

<sup>a</sup> School of Behavioral and Brain Sciences, Callier Advanced Hearing Research Center,  
The University of Texas at Dallas, 1966 Inwood Road, Dallas, TX 75235, USA

<sup>b</sup> Department of Speech and Hearing, Arizona State University, Tempe, AZ, USA

<sup>c</sup> Departments of Otolaryngology and Biomedical Engineering,  
University of North Carolina at Chapel Hill, NC State University in Raleigh, Chapel Hill, NC, USA

Accepted 7 April 2006

### Abstract

**Objective:** To compare two methods of minimizing cochlear implant artifact in cortical auditory evoked potential (CAEP) recordings.

**Methods:** Two experiments were conducted. In the first, we assessed the use of independent component analysis (ICA) as a pre-processing filter. In the second, we explored the use of an optimized differential reference (ODR) for minimizing artifacts.

**Results:** Both ICA and the ODR can minimize the artifact and allow measurement of CAEP responses.

**Conclusions:** When using a large number of recording electrodes ICA can be used to minimize the implant artifact. When using a single electrode montage an optimized differential reference is adequate to minimize the artifact.

**Significance:** The use of an optimized differential reference could allow cortical evoked potentials to be used in routine clinical assessment of auditory pathway development in children and adults fit with cochlear implants.

© 2006 International Federation of Clinical Neurophysiology. Published by Elsevier Ireland Ltd. All rights reserved.

**Keywords:** Cochlear implant; Cortical auditory evoked potential; P1; Artifact; Independent component analysis

### 1. Introduction

The latency and morphology of the cortical, auditory-evoked potential (CAEP) can provide information about the maturation of central auditory pathways (Ceponiene et al., 2002; Eggermont, 1988; Ponton et al., 1996, 2000; Sharma et al., 1997, 2002b, 2004). In a series of papers, we have documented the use of the CAEP as a measure of central auditory maturation in children who have received cochlear implants (CIs) and have suggested use of this measure in monitoring auditory pathway development in hearing-impaired patients (Sharma et al., 2002a,b,c, 2005). In normal hearing children, the latency of the P1 CAEP decreases systematically as age increases (Ponton et al.,

2002; Sharma et al., 2002b). For newborn infants the latency of the P1 can be as long as 300–400 ms. The latency can be as short as 50 ms in adults. Thus, the region of interest for the P1 is between 50 and 300 ms. Recording the CAEP in CI patients poses a unique problem in that implant devices, during stimulation, create electrical artifacts on the scalp, which interfere with identification of the CAEP (Sharma et al., 2002b; Singh et al., 2004). Several aspects of these electrical artifacts can be visualized by comparing the averaged CAEP records in Fig. 1 obtained using free-field acoustic stimulation with a normal-hearing child and a child fit with a CI. For the normal-hearing child the CAEP is dominated by the P1 neural response in a post-stimulus latency window of 50–300 ms. In the case of the CI user the record of the P1 response is obscured by a large magnitude (50  $\mu$ V) pedestal beginning slightly after the stimulus onset and ending slightly after the stimulus offset. This pedestal is

\* Corresponding author. Tel.: +1 214 905 3185; fax: +1 214 905 3146.  
E-mail address: pgilley@utdallas.edu (P.M. Gilley).

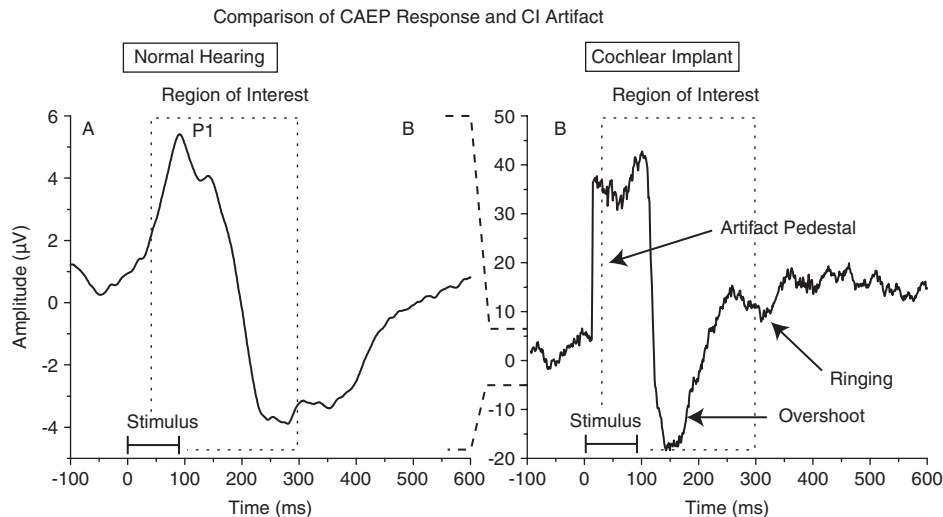


Fig. 1. (A) Typical CAEP response from a normal-hearing child aged 8 years. (B) CAEP response from a cochlear implanted user displaying a large stimulation artifact from the implant device. The region of interest for the P1 CAEP components are within the dotted lines, and the duration of the stimulus is shown with the bar above the abscissa. Note the different ordinate scales between panels A and B.

followed immediately by a larger negative-going overshoot and subsequent ringing of the recording amplifier filters. In addition, there is a low magnitude noise floor introduced throughout the entire record due to the ongoing background stimulation by the speech processor even during periods of low sound levels.

To a large extent, distribution of the artifact on the scalp is influenced by the type of cochlear implant device, its mode of stimulation (e.g. monopolar or bipolar coupling), and the surgical placement of the remote return electrode. The placement of the remote return electrode for monopolar stimulation varies widely across devices, being integrated into the stimulator package in the Clarion device but implemented as a separate electrode in the Nucleus and Med El devices. In our earlier work (e.g. Sharma et al., 2002b) we reported an artifact in about 12% of cases when using a contralateral mastoid as the reference electrode. In that earlier work, data were collected in large part from patients fit with the Nucleus 22 device, which uses bipolar stimulation. Devices running with bipolar electrodes in the cochlea produce substantially smaller artifact on the scalp as compared to the now commonly used monopolar-coupled electrodes. In fact, recent data collected in our laboratory have revealed a much greater incidence of the artifact problem from patients with devices using monopolar stimulation as described above. In general, the monopolar configuration will be the most common configuration used in the future, so the future incidence of artifact issues is likely to be very large in children receiving cochlear implant devices. Because the presence of the CI stimulation artifact diminishes the utility of the CAEP in children fit with implants, it would be useful to explore and understand the nature of the artifact in order to create methods of minimizing the artifact in CAEP recordings.

The scalp recorded EEG is assumed to be a linear, instantaneous mixture of multiple neural sources plus noise, and when multiple EEG epochs are averaged in response to a common auditory stimulus the CAEP reflects neuronal activity in response to that stimulus (Makeig et al., 2004; Nunez, 1981; Scherg and Von Cramon, 1986). In practice, most of the noise recorded in the EEG is minimized by averaging multiple EEG epochs in response to repeated stimulation. Because brain activity responding to the stimulus is assumed to be represented in each EEG trial, the resulting average should reveal the appropriate average evoked potential. Electrical activity generated from the implanted electrode array is not temporally random throughout the EEG recording because bipolar electrical pulses are generated with each presentation of the auditory stimulus. Therefore, the CI stimulation artifact, as well as the biologic response, are time-locked to the stimulus and are represented in the averaged response. Assuming that the recording system maintains linear operation throughout, one possible correction for this might be to use an acoustic stimulus that alternates in polarity on subsequent presentations throughout the recording, thus canceling the averaged stimulus artifact for an even number of trials. However, this is not possible in recordings from CI patients wearing their clinical processors as the speech processors do not encode the phase of the incoming acoustic stimulus. This approach would also require temporal synchronization of the external acoustic stimulus, the pulse train delivered by the processor, and the sampling clock of the recording system (Miller et al., 2000; van den Honert and Stypulkowski, 1986). This is an achievable goal using specialized hardware and software, but is beyond the capability available in most clinics.

A CI stimulation artifact will last for at least the duration of the stimulus. Given that the amplitude of the artifact can

be 5–10 times larger than the averaged evoked response, the artifact will mask a biologic response of interest that occurs within the time frame of the stimulus duration. We have used a 97 ms speech sound, /ba/, to elicit the CAEP in implant patients (Sharma, 2002a,b,c). It is reasonable to assume that shortening the speech stimulus would result in a shorter artifact—one that does not coincide with the region of interest for the P1. To determine if this is the case we compared CAEPs from a short duration (23 ms) vowel sound, 'uh', and a 97 ms speech sound, /ba/. As can be seen in Fig. 2, the duration of the artifact pedestal was shorter in the brief stimulus condition. However, the artifact did, in fact, overlap the early portion of the time region of interest because of filter ring. Limiting the amount of filter ring may be possible by changing the analog filter characteristics of the recording amplifiers (Andersen and Buchthal, 1970). However, the use of wide-band filters and higher sampling rates may also limit the feasibility of the CAEP as a clinical tool, because additional biologic artifacts at higher frequencies (e.g. muscle activity and fast ocular activity) often contaminate higher bandwidth recordings. The introduction of additional artifacts will increase the computational resources required to achieve a useful CAEP response and increase the time needed to retain useable EEG recordings. Obtaining a useful CAEP in a relatively short period of time is of great importance in a clinical setting, especially when limited recording time is an issue (e.g. recording from small children). The 23 ms signal used in this preliminary test is at the lower limit of duration for speech stimuli and still produced an artifact in the time region of interest. Thus, it would be best to look for other techniques to minimize the stimulus artifact.

Our experience has shown that, if not handled in a robust manner, the electrical artifact will either obscure the desired

biological response, or worse yet, be misinterpreted as a biological response. The later outcome is common when CAEP recordings are low-pass filtered at 30 Hz—a typical procedure when processing CAEP recordings. In this paper we examine two approaches for minimizing the two problems described above.

### 1.1. Post-processing analysis for removal of artifact

Several techniques have been proposed for removal of EEG artifacts that occur from biological sources such as ocular, muscle, and cardiac activity. A technique commonly used for artifact reduction is principal components analysis (PCA) (Casarotto et al., 2004; Croft and Barry, 2002; Jung et al., 2000a; Pantev et al., 2005; Vigario et al., 2000). PCA is a statistical technique that decorrelates data into a series of factors based upon the amount of variance explained. The first principal component explains the largest amount of variance in the original dataset, the second component the second largest amount of variance, and so on. However, because PCA only identifies orthogonal components based upon the variance of the data, this technique may not completely separate the biologic artifacts from the neural responses, and some loss of EEG data may occur when using this approach (Croft and Barry, 2002; Jung et al., 2000a,b). Ideally, a decomposition of underlying activity should maximize the independence of the sources contributing to the EEG activity and minimize the loss of EEG data that may be of interest after removal of the unwanted signals. Independent Component Analysis (ICA) has been proposed as a technique for achieving the required signal separation (Bell and Sejnowski, 1995; Delorme and Makeig, 2004; Jung et al., 2000a; Makeig et al., 1997, 2004; McKeown et al., 1998; Vigario et al., 2000).

The ICA model is a generative model that maximizes information from higher-order statistics (typically using an analysis of kurtosis or negentropy) to identify factors, or components, that are uncorrelated and mutually independent. Essentially, the ICA model first decorrelates the dataset using a PCA model (second order statistics). Next, an iterative process changes the weights and directions of the vectors in a mixing matrix until maximum independence is identified from the higher order statistics and the data converge. The results of this generative model are a set of components that represent the underlying structure of the data. Theoretically, each independent component represents the activation of one contributing source to the average evoked potential. Therefore, it should be possible to linearly subtract artifactual components from the ICA mixing matrix.

The ICA model must satisfy a series of criteria about the underlying sources. First, the sources are considered to be maximally independent; that is they are statistically uncorrelated with other sources. Second, the sources must have non-Gaussian distributions. Third, the sources should be, ideally, stationary (non-stationary ICA should be

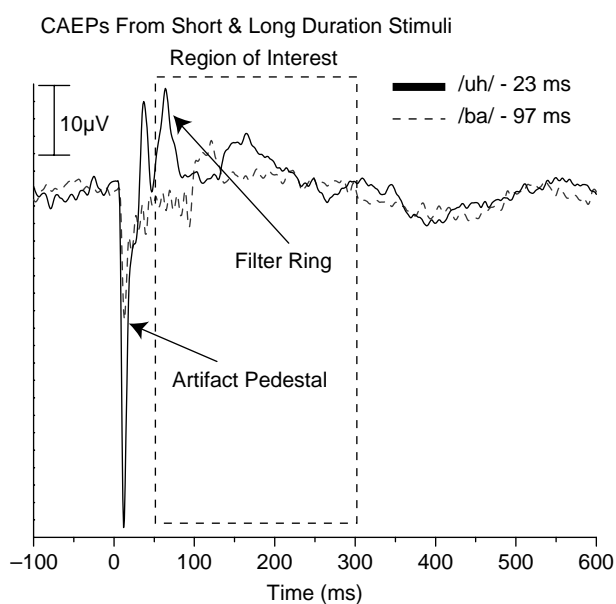


Fig. 2. Comparison of CAEP responses elicited by the short duration/uh/ and long duration/ba/speech sounds.

considered a separate problem). In the case of the CI stimulation artifact all of these criteria are satisfied. It is important to consider that these assumptions are strictly statistical in nature and do not rely on the physiologic or biologic nature of the signals to meet these criteria. The artifactual sources from the implanted device are independent, as they are generated by the implant array, and not by other neural sources. Further, the activity from the array is generated relative to one or more common electrodes, which correlates this activity and reduces the number of underlying components that are mutually independent. Most of the clinical processors worn by the patients utilize a single, common return electrode implanted at a remote location under the scalp. Because this electrode is common to each other electrode, the recorded activity is statistically correlated and, therefore, not independent. The separation of the components is then limited to the independence of the signals recorded on the scalp, which consists of the low-frequency pedestal and the high-frequency information from the biphasic pulses along the implanted electrode array, and is separated in the PCA in the first stages of ICA decomposition. The artifact is time-locked to the auditory stimulus, occurring at the same time in each EEG trial and, thus, is stationary and non-Gaussian in distribution. Based on the properties of the CI stimulation artifact in the EEG, ICA is a plausible technique for identifying and removing unwanted components in the EEG as a pre-processing step before averaging.

### 1.2. Optimized differential reference for removal of artifact

Data from a large number of channels (ranging from 16 to 64) must be collected in order to implement an ICA analysis. However, most audiology clinics do not have instrumentation to accomplish this type of analysis. Thus, it is necessary to explore techniques of artifact reduction, which could be implemented using a small number of recording channels. In the present study we explored a recording technique, the optimized differential reference technique (ODR), to minimize contribution of the artifact in the evoked potential recording. Based on observations from 32 to 64 channel recordings we established that the electrical activity generated by the implanted array is broadly distributed on the scalp and generally has a dipole distribution with peak magnitude levels near the active stimulation electrode(s) located within the cochlea and a common extracochlear return electrode located remotely beneath the scalp. Recalling that our object is to record a CAEP at Cz relative to a remote reference electrode (typically placed on the contralateral mastoid), we seek to minimize the artifact measured differentially at Cz by selecting a more optimal reference electrode site (Kornfield et al., 1985; McGill et al., 1982; Nilsson et al., 1988). There may be many such reference electrode sites on the scalp, which meet the criteria of (1) being located along an isopotential electrical artifact contour passing through Cz

and (2) being sufficiently far away from Cz to be electrically neutral to the CAEP events being recorded at Cz. In particular, we recorded from several reference-electrode sites around the forehead with the aim of determining the reference site that showed a null artifact (i.e. a location along the isopotential equal to that at Cz). If the spatial location of this isopotential could be estimated, then placing the reference electrode at this location should minimize the contribution of the artifact (McGill et al., 1982). In other words, we aimed to place our reference electrode at a location where differential recording would minimize the artifact.

### 1.3. Two experiments

In this study, we explored two methods to minimize the stimulation artifact during CAEP recordings. In Experiment 1 we applied ICA to the contaminated EEG from a group of CI users. In this analysis, multiple components in each recording were identified and attributed to the implanted device. After removing the unwanted signals, the EEG was recomputed and processed for evaluation of the CAEP. In Experiment 2 we explored the use of an optimized differential reference, i.e. where signals on an active electrode (Cz) were differentially recorded relative to a reference electrode located at various positions. The aim was to identify a reference location along the isopotential contour of the artifact appearing at Cz and, thus, minimize the artifact by recording differentially. Finally, we compared the CAEP obtained after removing the artifact using ICA to the CAEP recorded using the 'optimized differential reference technique' for artifact minimization. At issue was whether the two techniques to remove the CI stimulation artifact revealed a similar biological response.

## 2. Methods

### 2.1. Subjects

Subjects were 5 children aged 5.2–12.7 years (mean age = 10.46) who had been fitted with a cochlear implant. The children were selected for testing because in a previous visit to our laboratory their CAEP records had been obscured by an artifact. The children received their implants at ages ranging from 2.6 to 10.9 years (mean implant age = 6.5). Four subjects used Nucleus 24 devices with a monopolar configuration, and one subject (Subj B) used a Nucleus 22 device with a bipolar configuration. Three of the five subjects performed Experiments 1 and 2 on the same day. Subject A performed Experiment 1, 4 months after Experiment 2. Subject D performed Experiment 2, 4 months after Experiment 1.

## 2.2. Stimuli

The acoustic stimulus was a computer synthesized consonant-vowel syllable/ba/. Stimulus duration was 97 ms (see Sharma et al., 1997). The stimulus was presented with an interstimulus interval of 610 ms.

## 2.3. Evoked potential recording

Subjects were situated in a sound attenuated booth, in a comfortable chair, and allowed to watch a DVD movie of their choice. Audio levels from the DVD movie were turned off, and captioning was turned on. The speech sound was presented at a level of 70 DB SPL as measured at the subject's head location in the booth. The stimulus was presented through a loud speaker in the booth, placed at a 45° angle on the side of the CI, approximately 1.5 m from the subject.

For Experiment 1 the EEG was recorded using a 66-channel scalp electrode array (sintered Ag/AgCl, Neuroscan QuickCap) placed on the scalp according to the extended International 10–20 System for electrode placement. In some cases, one or more of the electrodes could not be used, because the electrode was directly over the implant transmission coil. The electrode (QuickCap) application took approximately 30 min. For Experiment 2, evoked responses were recorded from Cz, referenced to 6–13 different locations across the forehead. A separate channel was placed at the lateral canthus location of the eye contra-lateral to the implant (referenced to supra-orbit) for eye blink monitoring and on-line removal. Electrode application took approximately 10 min for the ODR montage.

In both experiments, continuous EEG was recorded using a 66-channel Synamps amplifier system (Compumedics-Neuroscan, El Paso, TX), with analog band-pass filter settings from 0.1 to 100 Hz, at a sampling rate of 1000 Hz, and an amplifier gain of 1000. Two recordings of approximately 300 trials were collected during the testing session, and saved to a computer for further analysis. The total testing time after electrode application was approximately 30 min.

## 2.4. Data analysis

For Experiment 1 each continuous EEG trace was visually analyzed for abnormal activity including extreme muscle activity, and extraneous noise. Sections of the EEG traces containing excess noise were blocked, and rejected from further analysis. The remaining EEG was divided into individual epochs around the onset of each stimulus presentation, with a 100 ms pre-stimulus interval and a 600 ms post-stimulus interval, resulting in approximately 300 trials with 701 sample points per trial for each recording. Epochs were baseline corrected to the average amplitude across the entire epoch inclusive of any artifact

occurring within the record. Eye-blinks were monitored on the separate eye channel, and epochs containing activity of  $\pm 100 \mu\text{V}$  were rejected from further analysis. After ICA analysis (described below), the two runs of 300 sweeps were averaged together to compute an average waveform for each subject.

For Experiment 2 each recording was baseline corrected to the average amplitude point of the waveform, and sweeps containing eye activity greater than  $\pm 100 \mu\text{V}$  in amplitude were rejected off-line. The two runs of 300 sweeps were averaged to compute a CAEP waveform for each subject.

## 2.5. Independent component analysis

The EEG files were imported in to the Matlab environment using the EEGLAB Toolbox (EEGLAB, San Diego, CA) under the public GNU license (Delorme and Makeig, 2004). ICA was performed on each EEG recording using the Infomax approach (Bell and Sejnowski, 1995). Independent component activations were projected to the scalp as isocontour maps for visual analysis, and each component was analyzed for kurtosis, Gaussianness, spectral power, variance explained (component weight), and amplitude duration in each trial of the EEG recording. Component activations were treated as CI artifact if they met the following criteria:

- (i) the onset of activity occurred at the onset of the auditory stimulus;
- (ii) the offset of activity occurred at the offset of the auditory stimulus (note: some components contained additional activity related to filter ringing after the offset of the stimulus, and this activity appeared as activation in the same component. If this was the case, and the initial activity met requirements (i) and (ii), then the secondary activity from the filter ringing was considered an artifactual component);
- (iii) the duration of the activity was constant throughout the duration of the auditory stimulus and
- (iv) scalp projections of the activity revealed a centroid on the side of the implanted device.

Components meeting these criteria were marked as CI artifact and linearly subtracted from the mixing matrix. The remaining components were then re-calculated to produce a filtered EEG dataset, and averaged to produce the CAEP.

## 3. Results

### 3.1. Experiment 1: artifact minimization using independent component analysis (ICA)

#### 3.1.1. Scalp maps of the CI stimulation artifact

Scalp maps of the averaged evoked activity from the evoked potential recordings revealed a scalp artifact

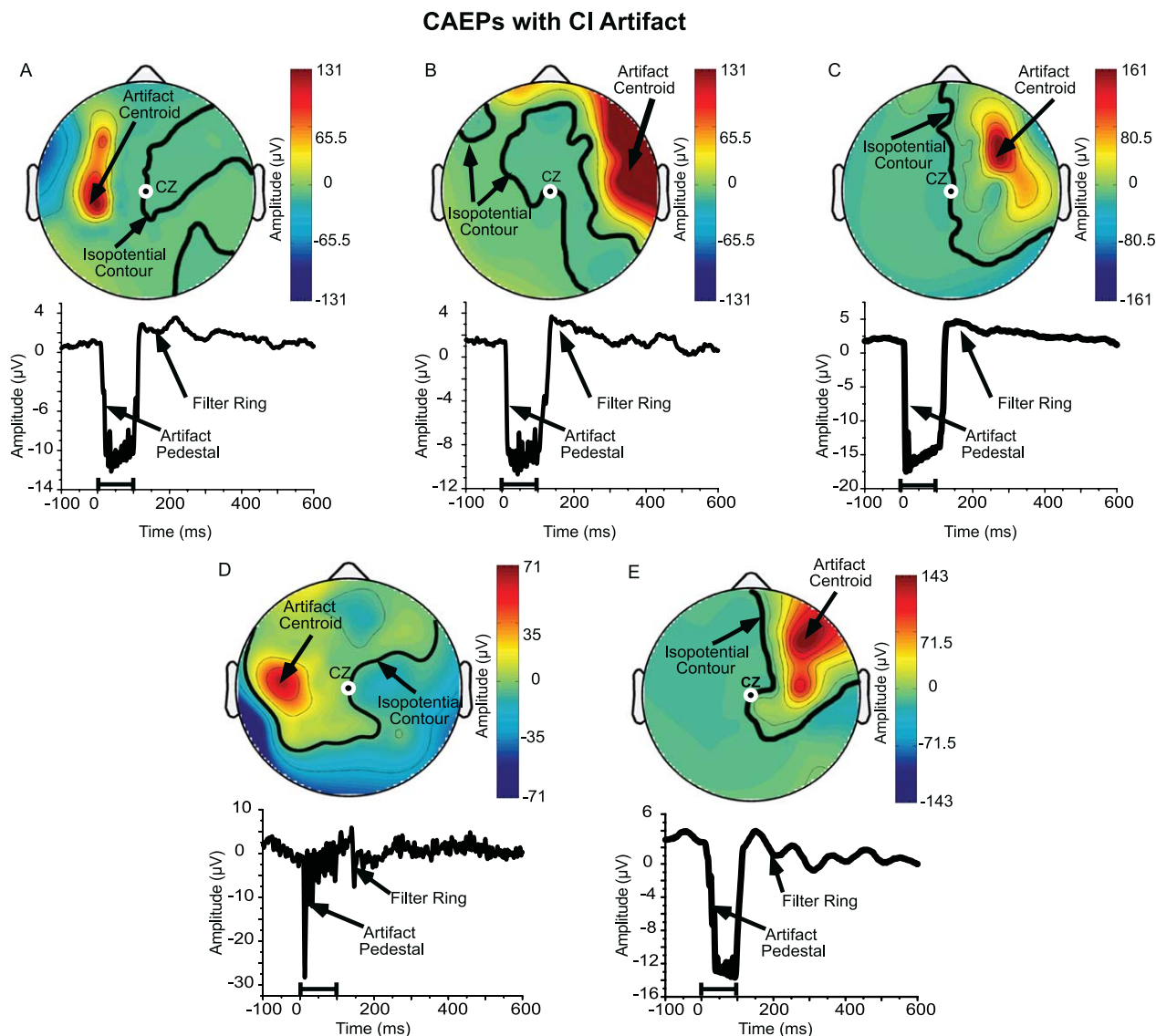


Fig. 3. Scalp maps and CAEP waveforms (at Cz) from Experiment 2. Each CAEP is represented by the spline-interpolated scalp projection at the center of the peak amplitude of the implant artifact. The isopotential contour passing through Cz is shown by the solid black line. The time-amplitude CAEP waveforms from Cz are shown below each scalp map. Each subject is designated with a label (A–E) and is consistent with the remaining figures.

distribution that concealed biologic activity in the time range of the CAEP (Fig. 3). In each case, the artifact was centered on the hemisphere of the CI device and peaked in the vicinity of the subcutaneous return electrode. Although, the artifact amplitude was much lower at the Cz electrode, which is typically used for CAEP recordings, than at sites near the implant, sufficient artifact was present to mask the biologic response.

### 3.1.2. ICA and artifact activations

Independent component analysis was performed on recordings from 5 CI patients using a 66-channel recording. At least two artifactual independent components, the artifact pedestal, the biphasic pulse, or the filter ringing, were identified in all patients. Fig. 4 shows the activity from the

independent components in all five subjects. As can be seen in Fig. 4, there is considerable variability across subjects for the scalp distribution of the components as well as for the general morphology of the component waveform. However, the scalp distribution of each component is generally centered near the implant.

After removing the artifactual components from the mixing matrix, CAEP responses were reconstructed. In all 5 subjects, the averaged CAEP contained a minimal artifact and the waveform morphology of the CAEP at the vertex (Cz) was similar to those of implanted subjects with little or no artifact in the CAEP (cf. Sharma et al., 2002a,b,c). Fig. 5 shows the reconstructed CAEP waveforms and scalp maps after artifact removal. A comparison of Figs. 3 and 5 reveals that the CAEP components are clearly evident in the region of interest where previously only the artifact was seen.

## Independent Components of the CI Artifact

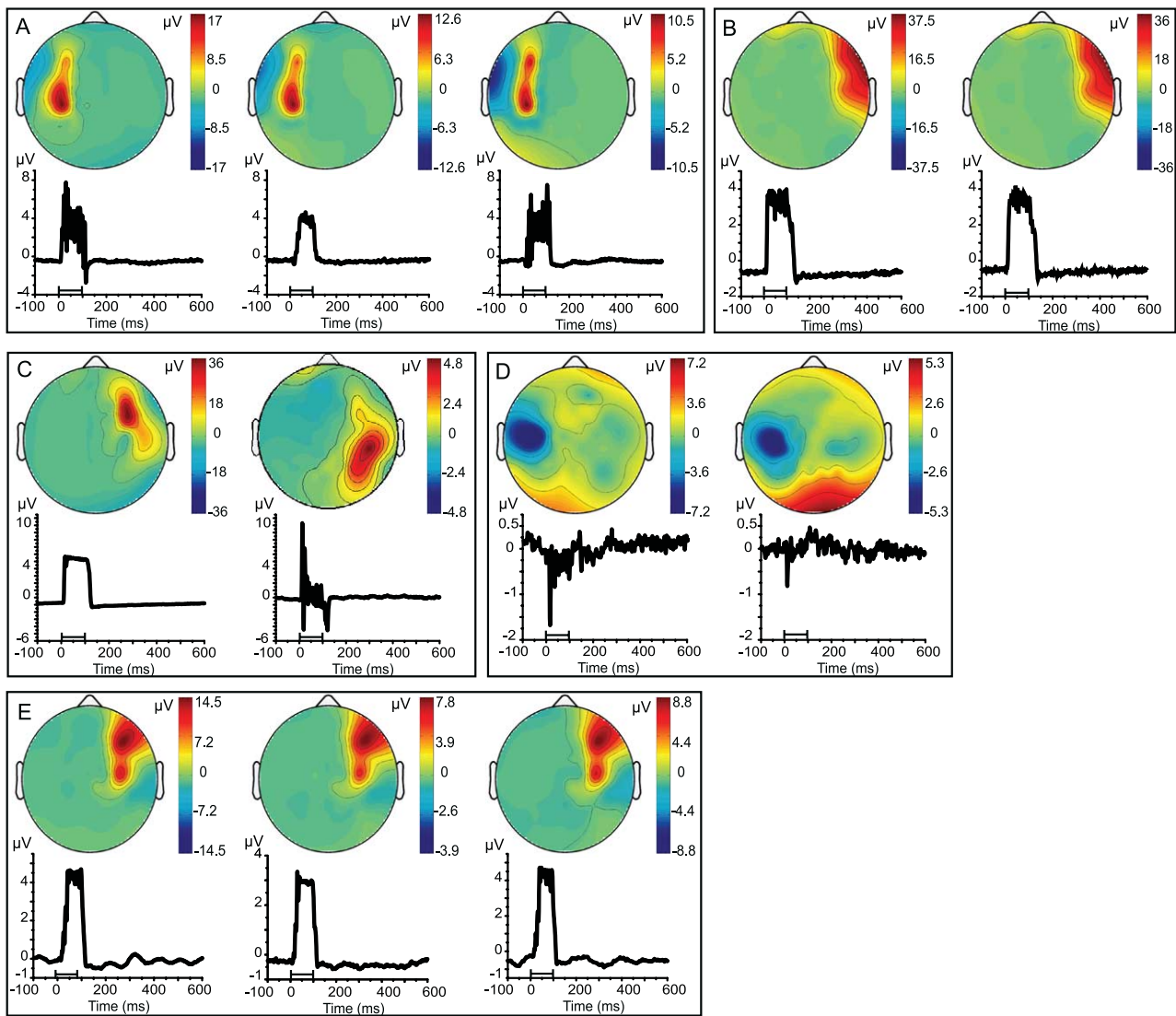


Fig. 4. Scalp maps and activations of the independent components (ICs) of the CI artifact for each subject (from Fig. 1). Each IC is represented by the IC waveform and the scalp projection of the component. Amplitudes are shown in microvolts and are calculated as the back projection to Cz. Each subject is designated with a label (A–E) and is consistent with the remaining figures.

### 3.2. Experiment 2: artifact minimization using an optimized differential reference

Based on the scalp maps computed from multichannel recordings we observed that in the scalp artifact distribution an isopotential contour would commonly extend from Cz and cross the forehead (Fig. 4). To evaluate the effect of placing the reference electrode near the Cz isopotential contour, we recorded individually from multiple reference sites across the forehead.

In Fig. 6, we show the variability of the residual artifact as a function of the placement of the reference electrode in a representative subject. The location of each reference electrode is represented on the head model and labeled with a letter corresponding to the CAEP response referenced to that location. In each of the recordings, Cz was used as

the active electrode and the labeled location as the reference. Beginning at location A the residual artifact is characterized by a negative pedestal followed by a positive overshoot. Moving from position A to the right the artifact reaches peak amplitude at D and then declines. It appears to reach a minimum in the vicinity of F and G and then begins to appear as a positive residual at H and I. The positions J, K and L were chosen to track along a possible isopotential contour toward Cz from the vicinity of G. Positions L and K show minimum residual artifact as would be expected; however, position J does not for unknown reasons. In this example, the best site for the reference electrode was at site K. The PI latency at site K was 160 ms.

In Fig. 7 CAEPs recorded with the reference located along the Cz isopotential contour are superimposed on the CAEPs generated from the ICA filtering procedure in

## CAEPs with Minimized CI Artifact

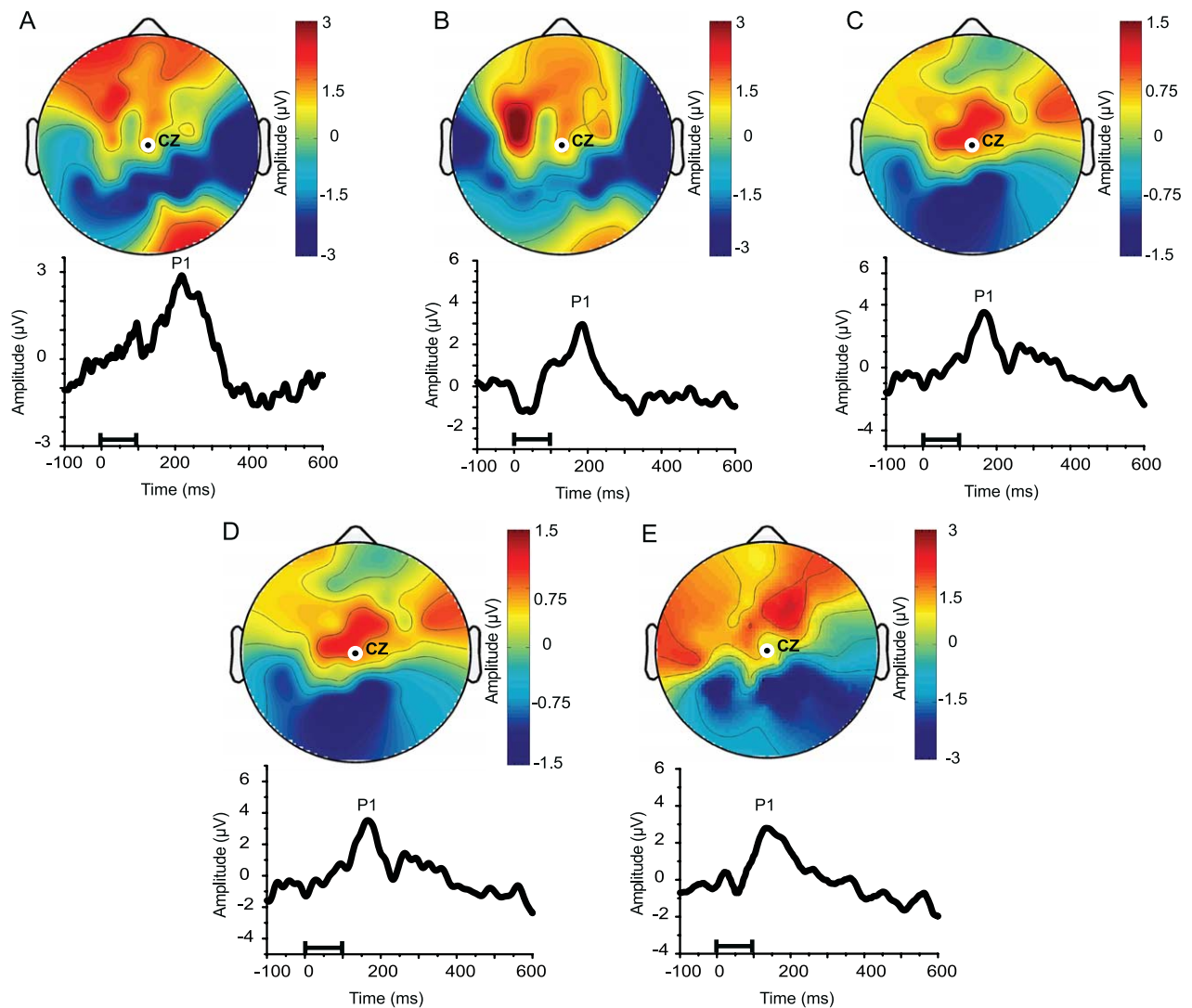


Fig. 5. Scalp maps and CAEP waveforms (at Cz) from Experiment 2 after the artifact ICs were removed. Each CAEP is represented by the spline-interpolated scalp projection at the center of the peak amplitude of the first robust, positive CAEP peak (P1). The averaged CAEP waveform at electrode Cz is shown below the scalp projections. Each subject is identified in the panel with a designated label (A–E) and is consistent for Fig. 4.

Experiment 1. The morphology of the two waveforms, within subjects, is very similar. In two cases (A and D) there are small differences in P1 latency. In these cases the two recording sessions were three months apart and the changes in latency are the expected consequence of the added experience with stimulation (Sharma et al., 2002c). Fig. 8 compares the mean latency and amplitude of the P1 between the ICA and ODR techniques. Paired *t*-tests of the latencies and amplitudes revealed no significant differences ( $P=0.66$  and  $0.33$ , respectively).

#### 4. Discussion

The CAEP could be a useful clinical tool for inferring the maturational status of the central auditory system in CI

patients if the stimulus artifact could be minimized. In the present study we examined two different techniques to minimize the contribution of the artifact to the CAEP response. In Experiment 1 we explored the use of ICA as a preprocessing filter for minimization of the artifact. ICA decomposition was performed on 66-channel recordings in five subjects. In all five cases at least two independent components attributed to the stimulus artifact were identified. In each case, linear subtraction of the artifactual components from the ICA mixing matrix resulted in CAEP responses containing typical amplitudes and latencies. Based on these results ICA is a viable tool for minimizing stimulus artifact when assessing the CAEP from a large number of recording electrodes.

One of the difficulties in using ICA for artifact removal is the correct identification of artifactual components from the

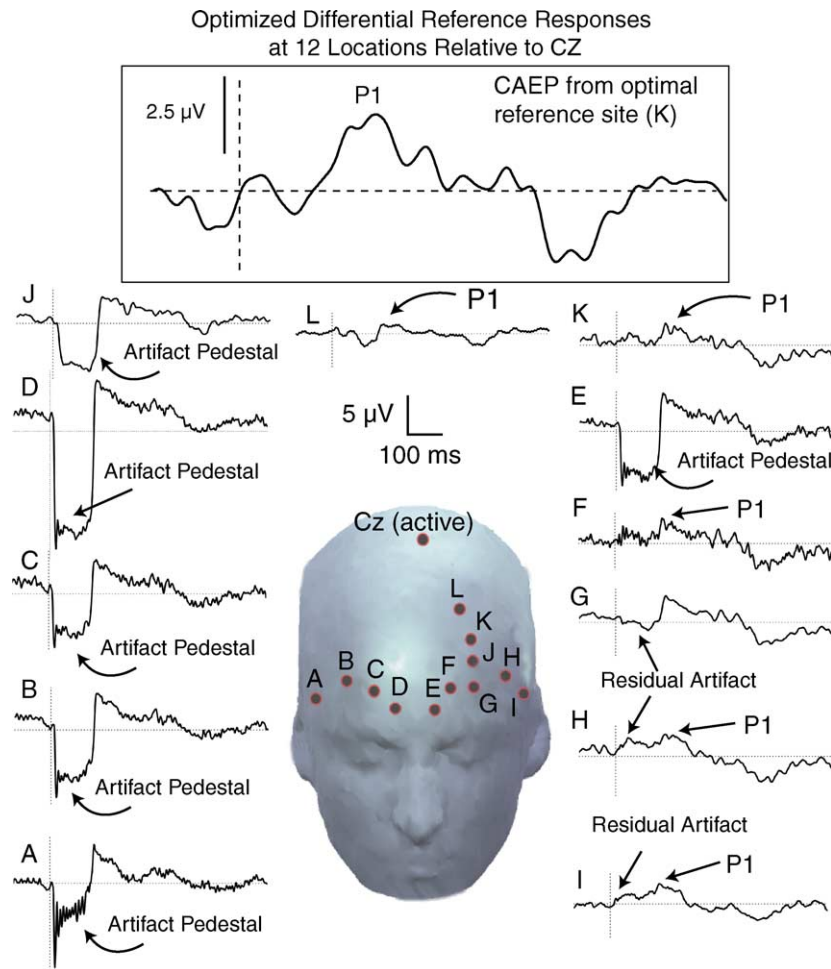


Fig. 6. CAEP responses from one representative subject as recorded using the optimized differential reference technique. The location of each reference electrode is represented on the head model, and each labeled with a letter corresponding to the CAEP response referenced to that location. In each of the recordings, Cz was used as the active electrode and the labeled location as the reference. The enlarged waveform at the top is from location K, and is displayed with a standard low-pass filter of 30 Hz (zero-phase shift, 12 DB/octave). This figure demonstrates the variable contribution of the artifact in a differential recording montage depending on the reference location.

analysis. In the present study, we implemented a fairly strict set of criteria for labeling such components. As a result, we were unable to completely remove the artifact, because components that contained stimulus-related activity but did not meet the criteria were not removed from the ICA mixing matrix. However, we were able to achieve results that minimized the artifact enough to reveal the biologic components of interest. There are several considerations about the nature of the stimulus artifact that may hinder identification of all artifactual components.

First, we make the assumption that the origin of activity in the recordings is the implanted electrode array. If this is the case, then the projection of the artifact may vary with the number of active electrodes in the array, the orientation of the active electrodes in the cochlea, and the location and orientation of the return electrode on the array. For example, a patient with 12–16 active electrodes, monopolar stimulation and a basal return electrode may show a broader dispersion of electrical activity on the scalp than a CI user

with 24 active electrodes using bipolar stimulation, i.e. when the return electrode is unique to a given electrode pair.

Second, we must assume that, because each patient's processor is individually programmed for best use, there will be individual differences in the electrical artifact. The speech processing algorithms used in CI devices employ several different strategies for electrode stimulation. Because the electrode stimulation patterns vary by processing strategy, the corresponding independent components could have different time-amplitude morphologies, weights, and distributions. Moreover, the pulses from the implanted array are not synchronous with the actual speech stimulus and/or the sampling of the averaging system. This can introduce significant jitter and variation from one record to another.

In Experiment 2 we utilized an optimized differential reference technique to identify a location on the scalp near the isopotential contour of the artifact that also crosses Cz. The aim was to determine whether placing a reference

## CAEPs from ODR and ICA

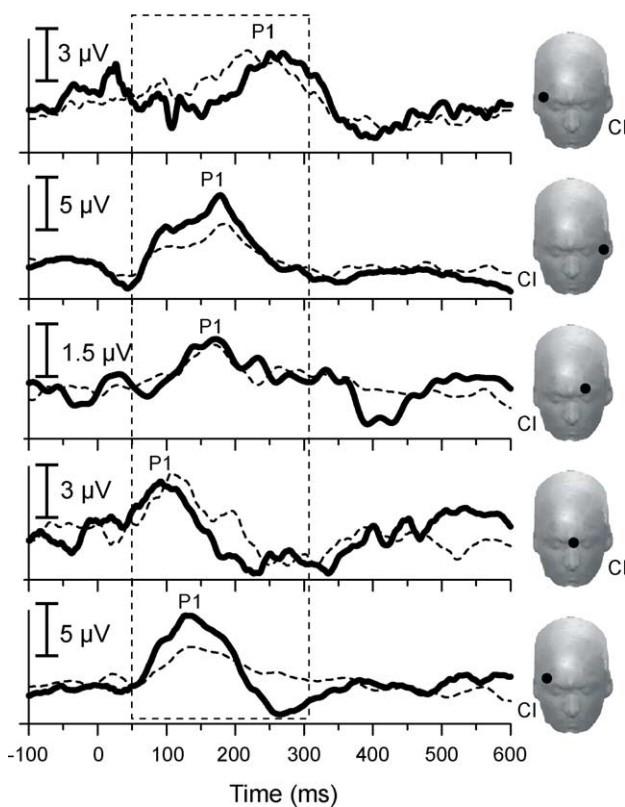


Fig. 7. CAEP responses from the ODR technique (thick, black line) and from the ICA filtering technique (thin, dotted line) for each of the subjects. The location of the reference electrode for the ODR condition is shown as a black dot on the head model to the right of each waveform. The test ear is indicated with the 'CI' label next to each head model.

electrode on or near this isopotential contour could minimize the contribution of the artifact to the CAEP response. Results from this experiment indicated that the artifact could, indeed, be minimized and a biological response could be measured. To further verify these results we compared the CAEP responses using the ODR technique to the responses minimized by ICA analysis. The P1 latencies and amplitudes were similar in each case suggesting that the optimized differential reference technique could be clinically useful. Although we found no

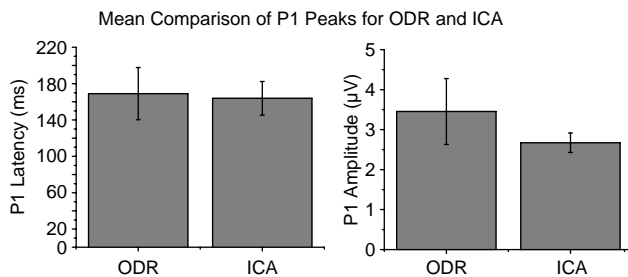


Fig. 8. Means and standard errors for (A) P1 latency and (B) P1 amplitude for all subjects.

significant differences in amplitude between the ICA and ODR responses, some minor variations in amplitude might be present. Such differences in amplitude might be accounted for by the use of a reference signal that is derived as a common average of all electrodes in the montage when using the ICA approach. In effect, the component of the P1 response contributed by biological signals on the reference will be spatially averaged over the entire cranium using the common average reference signal and would be expected to be smaller than the contribution from many single electrode sites. This common average reference signal is in contrast to the reference signal from a single electrode as with the ODR approach. One of the strengths of the optimized differential reference technique is that it is immune to the problem of time jitter as described above. Locating the correct isopotential location will allow the differential signal to minimize near zero, hence minimizing the artifact. These findings are consistent with findings from electromyographic and nerve conduction studies, which show that stimulus artifacts can be reduced by altering the orientation of either the stimulus or recording electrodes, as well as altering properties of the stimulus itself (Kornfield et al., 1985; McGill et al., 1982; Nilsson et al., 1988).

We can identify at least four problems that could constrain the use of the ODR technique. One is the number and location of electrodes needed to find an optimal reference point. If a large number of electrodes are necessary, then the clinical usefulness of the technique will be lessened. A second problem is how to obtain an objective measure of effectiveness of the technique. That is, once a small artifact is obtained, might another reference point yield an even smaller artifact? A third problem is how to judge the effect of even a minimal artifact in a recording, e.g. might a very minimal artifact still alter the measurements of interest or even be interpreted as a physiological response? Finally, we have observed that in some subjects the artifact isopotential contour passing through Cz may follow a very different trajectory from that typically seen across the forehead. Strategies to reliably and efficiently identify this situation and locate suitable alternative reference sites will be critical to successful clinical application of this approach. If these problems can be solved, then the optimized differential reference technique may allow CAEP studies to be used routinely to monitor objectively CNS maturation in newly implanted CI patients, especially the very young.

### Acknowledgements

We wish to thank the participants of this study; the children and their families for their enthusiastic participation. We wish to thank the two anonymous reviewers for their insightful comments and helpful suggestions. Comments from Arnaud Delorme and Julie Onton concerning

the use of ICA were very helpful in guiding this work. Funding provided by the National Institutes of Health: NIH-NIDCD R01-DC004552 and R01-DC006257.

## References

- Andersen VO, Buchthal F. Low noise alternating current amplifier and compensator to reduce stimulus artefact. *Med Biol Eng* 1970;8(5):501–8.
- Bell AJ, Sejnowski TJ. An information-maximization approach to blind separation and blind deconvolution. *Neural Comput* 1995;7(6):1129–59.
- Casarotto S, Bianchi AM, Cerutti S, Chiarenza GA. Principal component analysis for reduction of ocular artefacts in event-related potentials of normal and dyslexic children. *Clin Neurophysiol* 2004;115(3):609–19.
- Ceponiene R, Rinne T, Naatanen R. Maturation of cortical sound processing as indexed by event-related potentials. *Clin Neurophysiol* 2002;113(6):870–82.
- Croft RJ, Barry RJ. Issues relating to the subtraction phase in EOG artefact correction of the EEG. *Int J Psychophysiol* 2002;44(3):187–95.
- Delorme A, Makeig S. EEGLAB: an open source toolbox for analysis of single-trial EEG dynamics including independent component analysis. *J Neurosci Methods* 2004;134(1):9–21.
- Eggermont JJ. On the rate of maturation of sensory evoked potentials. *Electroencephalogr Clin Neurophysiol* 1988;70(4):293–305.
- Jung TP, Makeig S, Humphries C, Lee TW, McKeown MJ, Iragui V, Sejnowski TJ. Removing electroencephalographic artifacts by blind source separation. *Psychophysiology* 2000a;37(2):163–78.
- Jung TP, Makeig S, Westerfield M, Townsend J, Courchesne E, Sejnowski TJ. Removal of eye activity artifacts from visual event-related potentials in normal and clinical subjects. *Clin Neurophysiol* 2000b;111(10):1745–58.
- Kornfield MJ, Cerra J, Simons DG. Stimulus artifact reduction in nerve conduction. *Arch Phys Med Rehabil* 1985;66(4):232–5.
- Makeig S, Jung TP, Bell AJ, Ghahremani D, Sejnowski TJ. Blind separation of auditory event-related brain responses into independent components. *Proc Natl Acad Sci USA* 1997;94(20):10979–84.
- Makeig S, Debener S, Onton J, Delorme A. Mining event-related brain dynamics. *Trends Cogn Sci* 2004;8(5):204–10.
- McGill KC, Cummins KL, Dorfman LJ, Berlizot BB, Leutkemeyer K, Nishimura DG, Widrow B. On the nature and elimination of stimulus artifact in nerve signals evoked and recorded using surface electrodes. *IEEE Trans Biomed Eng* 1982;29(2):129–37.
- McKeown MJ, Makeig S, Brown GG, Jung TP, Kindermann SS, Bell AJ, Sejnowski TJ. Analysis of fMRI data by blind separation into independent spatial components. *Hum Brain Mapp* 1998;6(3):160–88.
- Miller CA, Abbas PJ, Brown CJ. An improved method of reducing stimulus artifact in the electrically evoked whole-nerve potential. *Ear Hear* 2000;21(4):280–90.
- Nilsson J, Ravits J, Hallett M. Stimulus artifact compensation using biphasic stimulation. *Muscle Nerve* 1988;11(6):597–602.
- Nunez PL. A study of origins of the time dependencies of scalp EEG: I. Theoretical basis. *IEEE Trans Biomed Eng* 1981;28(3):271–80.
- Pantev C, Dinnesen A, Ross B, Wollbrink A, Knief A. Dynamics of auditory plasticity after cochlear implantation: a longitudinal study. *Cereb Cortex* 2005.
- Ponton CW, Don M, Eggermont JJ, Waring MD, Masuda A. Maturation of human cortical auditory function: differences between normal-hearing children and children with cochlear implants. *Ear Hear* 1996;17(5):430–7.
- Ponton CW, Eggermont JJ, Kwong B, Don M. Maturation of human central auditory system activity: evidence from multi-channel evoked potentials. *Clin Neurophysiol* 2000;111(2):220–36.
- Ponton CW, Eggermont JJ, Khosla D, Kwong B, Don M. Maturation of human central auditory system activity: separating auditory evoked potentials by dipole source modeling. *Clin Neurophysiol* 2002;113(3):407–20.
- Scherg M, Von Cramon D. Evoked dipole source potentials of the human auditory cortex. *Electroencephalogr Clin Neurophysiol* 1986;65(5):344–60.
- Sharma A, Kraus N, McGee TJ, Nicol TG. Developmental changes in P1 and N1 central auditory responses elicited by consonant–vowel syllables. *Electroencephalogr Clin Neurophysiol* 1997;104(6):540–5.
- Sharma A, Dorman MF, Spahr A, Todd NW. Early cochlear implantation in children allows normal development of central auditory pathways. *Ann Otol Rhinol Laryngol Suppl* 2002a;189:38–41.
- Sharma A, Dorman MF, Spahr AJ. A sensitive period for the development of the central auditory system in children with cochlear implants: implications for age of implantation. *Ear Hear* 2002b;23(6):532–9.
- Sharma A, Dorman MF, Spahr AJ. Rapid development of cortical auditory evoked potentials after early cochlear implantation. *Neuroreport* 2002c;13(10):1365–8.
- Sharma A, Tobey E, Dorman M, Martin K, Gilley PM, Kunkel F. Central auditory maturation and babbling development in infants with cochlear implants. *Arch Otolaryngol Head Neck Surg* 2004;130(5):511–6.
- Sharma A, Martin K, Roland P, Bauer P, Sweeny M, Gilley P, Dorman M. P1 latency is a biomarker for central auditory development in children with hearing impairment. *J Am Acad Audiol* 2005;16(8):564–73.
- Singh S, Liasis A, Kaukab R, Luxon L. Short Report: methodological considerations in recording mismatch negativity in cochlear implant patients. *Cochlear Implants Int* 2004;5(2):76–80.
- van den Honert C, Stypulkowski PH. Characterization of the electrically evoked auditory brainstem response (ABR) in cats and humans. *Hear Res* 1986;21(2):109–26.
- Vigario R, Sarela J, Jousmaki V, Hamalainen M, Oja E. Independent component approach to the analysis of EEG and MEG recordings. *IEEE Trans Biomed Eng* 2000;47(5):589–93.